Inorganic Chemistry
Article
pubs.acs.org/IC

Specific Interaction between Uranium Anionic Complexes and the Cations of Bis(trifluoromethylsulfonyl)imide Based Ionic Liquids

Céline Cannes,*[†] Claire Le Naour,[†] Philippe Moisy,[‡] and Philippe Guilbaud[‡]

[†]Institut de Physique Nucléaire, CNRS, Univ. Paris-Sud 11, 91406 Orsay Cedex, France
[‡]CEA, Nuclear Energy Division, Radiochemistry & Processes Department, 30207 Bagnols sur Cèze, France

Ⓢ *Supporting Information*

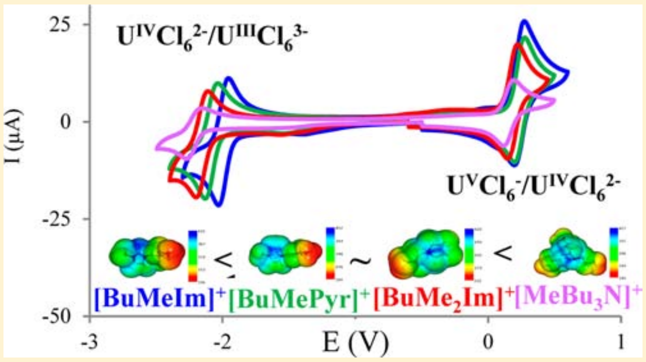

ABSTRACT: The redox properties of uranium(IV) hexachloro complex have been investigated with a glassy carbon electrode in four bis(trifluoromethylsulfonyl)imide (Tf_2N^-) based ionic liquids (ILs): the 1-butyl-3-methylimidazolium ($[BuMeIm]^+$), the 1-butyl-2,3-dimethylimidazolium ($[BuMe_2Im]^+$), the *N*-butylmethylpyrrolidinium ($[BuMePyr]^+$), and the tributyl-methylammonium ($[MeBu_3N]^+$). The cyclic voltammetric analysis has revealed two main redox systems: $U^{V}Cl_6^{-}/U^{IV}Cl_6^{2-}$ around 0.2 V and $U^{IV}Cl_6^{2-}/U^{III}Cl_6^{3-}$ around −2 V. The formation of $U^{V}Cl_6^{-}$, a non-dioxo uranium(V) species, can then be observed at the electrode in $[Tf_2N]^-$ based ILs. This work also provides evidence of a specific interaction between the uranium anionic species and the IL cations because the standard potentials of both redox couples depend on the IL. The interaction extent has been evaluated by comparison of the IL cation number associated with the uranium anionic complex. For that purpose, the standard potentials of both systems have been measured in the less interacting medium $[MeBu_3N][Tf_2N]$ as a function of the $[BuMeIm]^+$, $[BuMe_2Im]^+$, and $[BuMePyr]^+$ concentration. Predominance diagrams for uranium hexachloro complexes, analogous to the Pourbaix diagram, have then been built in $[MeBu_3N][Tf_2N]$ depending on the IL cations concentration. The exploitation of these diagrams leads to the conclusion that the interaction is function of the charge of the uranium hexachloro complex ($U^{V}Cl_6^{-} < U^{IV}Cl_6^{2-} < U^{III}Cl_6^{3-}$) and the IL cation ($[BuMe_2Im]^+ < [BuMePyr]^+ < [BuMeIm]^+$). The influence of the IL cation could be correlated to the size and the electropositivity of the IL cation. The association would occur by H-bonding and electrostatic interaction. Ab initio calculations were also carried out to evaluate the strength of the interaction between the anionic uranium(IV) chloro complex and the IL cations. The results show that $[BuMeIm]^+$ interacts the most and $[MeBu_3N]^+$ the least with $U^{IV}Cl_6^{2-}$, and the magnitude of the interaction is comparable for $[BuMe_2Im]^+$ and $[BuMePyr]^+$.

■ INTRODUCTION

Ionic liquids (ILs), composed of an organic bulky cation and an organic or inorganic anion, are liquid below 100 °C.[1,2] They have recently gained growing interest because of their unique properties such as low vapor pressure, nonflammability, good electrical conductivity, wide electrochemical window, and ability to solubilize a broad range of organic and inorganic compounds.[3,4] One of the main attractive advantages of these media is the possibility to fine-tune their physicochemical properties by a judicious choice of the anion/cation combination.[5,6] Because of their ionic character, ILs can be compared with the molten salts, composed of inorganic salts. Because molten salts present wide electrochemical windows, high conductivities, and high solubilities for metal salts, they are considered attractive media for metal electrodeposition.[7] However, their main drawbacks are the very high temperature conditions (up to 1000 °C) and their corrosion aspect. Therefore, ILs, which are nonvolatile and noncorrosive and operate at low temperature, appear to be good candidates to replace both organic solvents and high-temperature molten salts in many applications: synthesis, polymerization, catalysis, or electrochemistry.[8−14] ILs are investigated as possible media for actinide separation in nuclear fuel reprocessing.[14] However, the use of ILs in efficient actinide separation processes first requires fundamental data on the physicochemical properties of actinides in ILs. Reviews report physicochemical data on lanthanides and actinides in ILs.[15,16]

In addition, ILs can interact with solutes by H-bonding, π−π, or electrostatic effects in a way different from what is observed in conventional molecular solvents. Solvation has a direct effect on the chemical reactivity and redox properties, including both thermodynamical and kinetic parameters. For example, it has already been proven that ion pairing between transition metals and ILs leads to changes in the redox potential, catalytic activity, and reaction pathways.[17−21] Solvation effects on the electrochemical behavior in ILs are also reported for many organic compounds[22−30] and for dioxygen.[31−39] They are

Received: June 10, 2013
Published: September 10, 2013

Scheme 1. Cation Chemical Formulas of Selected Ionic Liquids

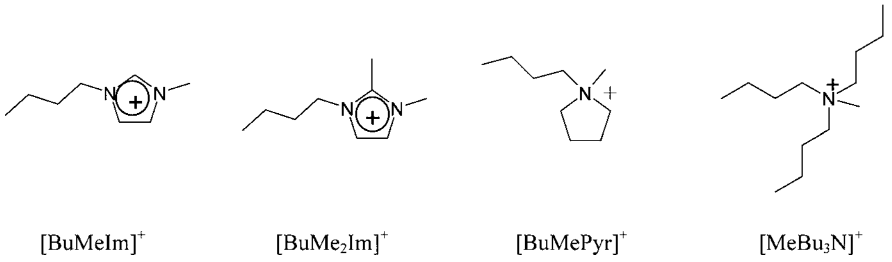

explained by the formation of strong ion pairing between the IL cation and the negatively charged electrogenerated species. It seems then essential to study the interaction of ILs with the solutes before selecting the best combination anion/cation for a specific application.

For some years, our work has been focused on the structure, solvation, and redox properties of $An^{IV}Cl_6^{2-}$ (An = U; Np; Pu) complexes in ILs based on the bis(trifluoromethylsulfonyl)-imide anion ($[(CF_3SO_2)_2N]^-$; $[Tf_2N]^-$).[40−43] Our results showed that the octahedral structure of actinide(IV) complexes in the solid state is maintained in the studied ILs and that the complexes are stable with respect to hydrolysis. The hexachloro Np(IV) and Pu(IV) complexes are electrochemically inert in the 1-butyl-3-methylimidazolium IL with a glassy carbon electrode. However, the voltammetric analysis of $U^{IV}Cl_6^{2-}$ revealed two redox couples in the 1-butyl-3-methylimidazolium ($[BuMeIm]^+$), the 1-butyl-2,3-dimethylimidazolium ($[BuMe_2Im]^+$), and the methyl-tributylammonium ($[MeBu_3N]^+$) bis(trifluoromethylsulfonyl)imide ILs: $U^VCl_6^-/U^{IV}Cl_6^{2-}$ and $U^{IV}Cl_6^{2-}/U^{III}Cl_6^{3-}$. Moreover, depending on the IL, shifts are observed on the redox potentials of $U^{IV}Cl_6^{2-}$, and they have been related to a specific interaction between uranium anionic species and the IL cations.[40] In the continuation of this work, the solvation of the $U^{IV}Cl_6^{2-}$ complex has been studied in three selected ILs based on the $[Tf_2N]^-$ anion.[43] Spectroscopic and electrochemical measurements have allowed us to show the interaction by hydrogen bonding between the chlorides of U(IV) anionic species and the IL cations. The hydrogen of the IL cation involved in the bonding has been identified and the strength of the interaction proved to vary in the following order: $[MeBu_3N]^+ \approx [BuMe_2Im]^+ \ll [BuMeIm]^+$.

Our goal is then to evaluate the interaction of IL cations and the uranium anionic species at the +III, +IV, and +V oxidation state. A molecular dynamic study has been already reported on the $U^{III}Cl_6^{3-}$, $U^{IV}Cl_6^{2-}$, and $U^VCl_6^-$ solvation in the ILs $[BuMeIm][Tf_2N]$ and $[MeBu_3N][Tf_2N]$.[44] The results have shown that it depends both on the IL and the charge of the uranium complex, being related to the oxidation state of the uranium. In both ILs, the solvation of uranium anionic complexes consists of an “onion” type alternation of solvent ions with a first solvation sphere essentially cationic (7.6, 5.5, and 4.6 in $[BuMeIm][Tf_2N]$ and 6.9, 5.2, and 4.1 in $[MeBu_3N][Tf_2N]$ for $U^{III}Cl_6^{3-}$, $U^{IV}Cl_6^{2-}$ and $U^VCl_6^-$, respectively). This work has also shown that the interactions between IL cations and uranium complexes occur by H-bonding. Moreover, the calculations have revealed that the three studied uranium complexes are better solvated by $[BuMeIm][Tf_2N]$ than $[MeBu_3N][Tf_2N]$. This difference of ion pairing extent for a given uranium species has been correlated to the size of the IL cation.

Since cyclic voltammetry is a powerful technique to analyze species at different oxidation states,[45] this technique has been used to determine the specific interactions between the uranium (III, IV, V) hexachloro complexes and various IL cations. The cations of Tf_2N-based ILs, $[BuMeIm]^+$, $[BuMe_2Im]^+$, $[MeBu_3N]^+$, and $[BuMePyr]^+$, are presented Scheme 1. The $[BuMePyr]^+$ cation stands for *N*-butylmethylpyrrolidium cation and is added to the IL cations selected because of its nonaromatic ring.

■ EXPERIMENTAL SECTION

Chemical Reagents and Synthesis. The ILs $[BuMeIm][Tf_2N]$, $[BuMe_2Im][Tf_2N]$, $[BuMePyr][Tf_2N]$, and $[MeBu_3N][Tf_2N]$ are commercially available (Solvionic, purity >99.9%) and were used without further purification. The density (at 20 °C) and the viscosity (at 25 °C) values were provided by Solvionic. The electrochemical window is systematically measured by cyclic voltammetry to control the purity. The chloride salts [BuMeIm]Cl (Solvionic), $[BuMe_2Im]Cl$ (Solvionic), [BuMePyr]Cl (Solvionic), and $[MeBu_3N]Cl$ (Fluka) are also commercially available (purity 98%) and were used without further purification. Whatever the IL, the water concentration measured by coulometric Karl Fischer titration was found to be from 100 ± 50 ppm (at the beginning of the electrochemical experiment) to 500 ± 100 ppm (at the end of the experiment).

$[Cation]_2[UCl_6]$ complexes, where $Cation^+$ is $BuMeIm^+$, $BuMe_2Im^+$, $BuMePyr^+$, or $MeBu_3N^+$, were prepared according to the procedure described in ref 40: they were obtained by precipitation from U(IV) solutions in 10 M HCl in the presence of a slight excess of the corresponding [Cation]Cl. The precipitates were washed with cold acetone saturated with argon and dried under reduced pressure at room temperature. The initial U(IV) solutions were prepared by dissolution of uranium metal in concentrated HCl. The solid hexachloro uranium(IV) complexes ($[Cation]_2UCl_6$) are described without a water molecule in their crystallographic structure.[46]

The ILs, chloride salts, and uranium compounds were stored in an argon-filled drybox. The samples were prepared and stored in the drybox. All complexes are well soluble under gentle heating in the studied ILs.

Electrochemical Devices. The electrochemical experiments were carried out with an Autolab PGSTAT30 device. A commercial three-electrode thermostatted Pyrex electrochemical cell (V = 3 mL) was used with a glassy carbon disk working electrode (GC, 0.07 cm^2, from Radiometer) and a Pt wire counter electrode. The working electrode was polished on emery paper with different granulometry sizes just prior to use. The reference electrode was prepared by immersing Ag wire in a 0.01 M solution of $Ag[CF_3SO_3]$ in $[BuMeIm][Tf_2N]$. The reference solution was placed in a glass liquid junction protection tube with a fine porosity frit (from Radiometer). All potentials are reported with respect to this reference. Under the experimental conditions described above, the values measured for the reference redox system Fc^+/Fc at 60 °C are −0.395 V in $[BuMeIm][Tf_2N]$, −0.394 V in $[BuMePyr][Tf_2N]$, −0.39 V in $[BuMe_2Im][Tf_2N]$, and −0.37 V in $[MeBu_3N][Tf_2N]$. The cell was deaerated with argon (O_2 < 0.1 ppm and H_2O < 0.5 ppm) 30 min before the measurements. Argon was also sparged into the cell during the electrochemical data acquisition. The electrochemical measurements were performed at 25 ± 1 °C and 60 ±

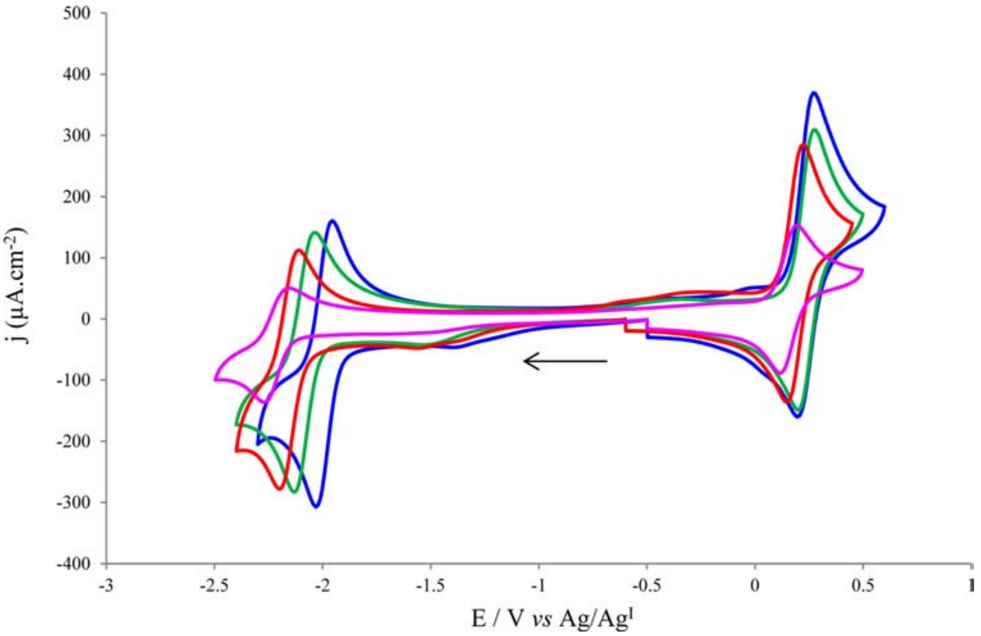

Figure 1. Cyclic voltammograms of a $[\mathrm{Cation}]_2[\mathrm{UCl_6}]$ 0.01 M solution in $[\mathrm{Cation}][\mathrm{Tf_2N}]$ with a GC electrode at 60 °C; $\nu = 0.1\ \mathrm{V\ s^{-1}}$. $[\mathrm{Cation}]^+ = [\mathrm{BuMeIm}]^+$ (blue), $[\mathrm{BuMePyr}]^+$ (green), $[\mathrm{BuMe_2Im}]^+$ (red), or $[\mathrm{MeBu_3N}]^+$ (purple).

1 °C, the temperature being controlled with a "Polystat 5" thermostat. The ohmic drop (*iR*) is compensated for all voltammograms by measuring the resistance *R* by impedance spectroscopy at the open circuit potential.

Electrochemical Protocol To Build the Predominance Diagram of the Uranium Hexachloro Complexes. The specific interaction between the IL cation and the uranium anionic species observed by voltammetry has been considered in terms of the number of IL cations in the first coordination sphere. If strong ion pairing occurs with IL cations, association reactions can be taken into account for each complex (eqs 1−3) without consideration of an eventual interaction of the uranium anionic species with the IL anions.

$$\mathrm{U^{V}Cl_6}^- + x\mathrm{L}^+ \rightleftarrows \mathrm{U^{V}Cl_6L_x}^{(x-1)} \qquad K_x^{\mathrm{V}} \tag{1}$$

$$\mathrm{U^{IV}Cl_6}^{2-} + y\mathrm{L}^+ \rightleftarrows \mathrm{U^{IV}Cl_6L_y}^{(y-2)} \qquad K_y^{\mathrm{IV}} \tag{2}$$

$$\mathrm{U^{III}Cl_6}^{3-} + z\mathrm{L}^+ \rightleftarrows \mathrm{U^{III}Cl_6L_z}^{(z-3)} \qquad K_z^{\mathrm{III}} \tag{3}$$

where L^+ stands for the IL cations present in the first coordination sphere of the anionic uranium species.

The association constants can then be expressed as follows:

$$K_x^{\mathrm{V}} = \frac{[\mathrm{UCl_6L_x}^{x-1}]}{[\mathrm{UCl_6}^-][\mathrm{L}^+]^x} \tag{4}$$

$$K_y^{\mathrm{IV}} = \frac{[\mathrm{UCl_6L_y}^{y-2}]}{[\mathrm{UCl_6}^{2-}][\mathrm{L}^+]^y} \tag{5}$$

$$K_z^{\mathrm{III}} = \frac{[\mathrm{UCl_6L_z}^{z-3}]}{[\mathrm{UCl_6}^{3-}][\mathrm{L}^+]^z} \tag{6}$$

Considering these chemical reactions, the oxidation and the reduction of uranium(IV) with monoelectronic transfer can be rewritten according to eqs 7 and 8.

$$\mathrm{U^{IV}Cl_6L_y}^{(y-2)} + (x-y)\mathrm{L}^+ \rightarrow \mathrm{U^{V}Cl_6L_x}^{(x-1)} + 1\mathrm{e}^- \tag{7}$$

$$\mathrm{U^{IV}Cl_6L_y}^{(y-2)} + 1\mathrm{e}^- + (z-y)\mathrm{L}^+ \rightarrow \mathrm{U^{III}Cl_6L_z}^{(z-3)} \tag{8}$$

The Nernst equation associated with the redox eq 7 can be written as the following:

$$E = E^0_{(\mathrm{V;IV})} + 2.303\frac{RT}{F}\log\left\{\frac{[\mathrm{U^V}]}{[\mathrm{U^{IV}}][\mathrm{L}]^{x-y}}\right\} \tag{9a}$$

$$E = E^0_{(\mathrm{V;IV})} + 2.303\frac{RT}{F}(y-x)\log[\mathrm{L}] + 2.303\frac{RT}{F}\log\left\{\frac{[\mathrm{U^V}]}{[\mathrm{U^{IV}}]}\right\} \tag{9b}$$

The standard potential is defined as

$$\begin{aligned} E'^0 &= E^0_{(\mathrm{V;IV})} + 2.303\frac{RT}{F}(y-x)\log[\mathrm{L}] \\ &= E^0_{(\mathrm{V;IV})} + 2.303\frac{RT}{F}(x-y)\mathrm{pL} \end{aligned} \tag{9c}$$

In the same way, the Nernst equation associated with the redox eq 8 can be written as

$$E = E^0_{(\mathrm{IV;III})} + 2.303\frac{RT}{F}\log\left\{\frac{[\mathrm{U^{IV}}][\mathrm{L}]^{z-y}}{[\mathrm{U^{III}}]}\right\} \tag{10a}$$

$$E'^0 = E^0_{(\mathrm{IV;III})} + 2.303\frac{RT}{F}(y-z)\mathrm{pL} \tag{10b}$$

According to the above equations, the determination of the coefficients *x*, *y*, and *z* will allow one to estimate the number of IL cations (L^+) in the coordination sphere of U(V), U(IV), and U(III) anionic hexachloro complexes. This can be done by measuring the variation of the standard redox potentials as a function of the IL cation concentration ($\mathrm{pL} = -\log[\mathrm{L}^+]$). The standard potential can be calculated from the half-sum of the anodic and cathodic peak potential ($E_{\mathrm{p/2}}$) measured by cyclic voltammetry (eq 11).

$$E_{\mathrm{p/2}} = \frac{E_{\mathrm{pa}} + E_{\mathrm{pc}}}{2} = E^0 + \frac{RT}{F}\log\left(\left(\frac{D_{\mathrm{red}}}{D_{\mathrm{ox}}}\right)^{1/2}\right) \tag{11}$$

In ILs, differences in the values of the diffusion coefficients of the reductor (D_{red}) and of the oxidant (D_{ox}) have been observed.[31,39] However, the studied system was $\mathrm{O_2/O_2}^{\bullet-}$. Because of the negative charge of $\mathrm{O_2}^{\bullet-}$, the interactions of the IL cations are much stronger with the superoxide than with the neutral molecule $\mathrm{O_2}$. This affects the diffusion coefficients. In the case of uranium hexachloro complexes, whatever the oxidation state, the species are bulky. Although the

Table 1. IL Viscosity (ν), IL Density (d), Concentration of the IL Ions, Anodic Peak Intensities (I_{pa}), Cathodic Peak Intensities (I_{pc}), and Standard Potential (Estimated by $E_{p/2}$) Measured by Cyclic Voltammetry for $[\mathrm{Cation}]_2[\mathrm{UCl}_6]$ (0.01 M) Solution in [Cation]$[\mathrm{Tf_2N}]$ at 60°C and 0.1 V s^{-1}

IL cation	ν (cP) at 25 °C	d at 20 °C	IL ion concn (mol L^{-1})	I_{pa} (μA) for U^{V}/U^{IV}	I_{pc} (μA) for U^{IV}/U^{III}	$E_{p/2}$ (V) for U^{V}/U^{IV}	$E_{p/2}$ (V) for U^{IV}/U^{III}
$[\mathrm{BuMeIm}]^+$	61	1.429	3.38	22.2	17.9	0.237	−1.993
$[\mathrm{BuMePyr}]^+$	84	1.41	3.33	19	16.7	0.241	−2.087
$[\mathrm{BuMe_2Im}]^+$	155	1.437	3.31	16.5	15.9	0.187	−2.156
$[\mathrm{MeBu_3N}]^+$	593	1.26	2.62	8.5	7.4	0.158	−2.214

coordination sphere of the oxidant and the reductor differ by the number of the IL cation, the difference in size of involved complexes is expected to be less marked than in the case of $O_2/O_2^{\bullet-}$. Therefore, the diffusion coefficients of the uranium(III, IV, V) hexachloro complexes have been assumed to be almost equal, and E^0 was calculated according to eq 12.

$$E_{p/2} = \frac{E_{pa} + E_{pc}}{2} = E^0 \tag{12}$$

To measure the variation of the potential standard as a function of the IL cation concentration, the solvent has to be an "inert" or "poorly-interacting" medium. Because $[\mathrm{MeBu_3N}]^+$ interacts with the uranium anionic species less than $[\mathrm{BuMeIm}]^+$,[43,44] $[\mathrm{MeBu_3N}][\mathrm{Tf_2N}]$ has been selected as the "poorly-interacting" medium. The standard apparent redox potentials for the U^{V}/U^{IV} and U^{IV}/U^{III} systems are thus measured by cyclic voltammetry for a $U^{IV}Cl_6^{2-}$ (0.01 M) solution in $[\mathrm{MeBu_3N}][\mathrm{Tf_2N}]$ in the presence of varying amounts of $[\mathrm{BuMeIm}]^+$, $[\mathrm{BuMePyr}]^+$, or $[\mathrm{BuMe_2Im}]^+$.

Electrostatic Potential Calculations. All molecule structures were fully optimized using Gaussian03[47] at the Hartree−Fock level using the 6 31+G** basis set. Electrostatic potential calculations were performed at the same level using the Merz−Kollman method.[48] Surfaces were represented using Molekel 5.4[49] mapping the calculated electrostatic potential at the accessible anion surface with an anion probe radius varying between 1.2 and 2.0 Å in order to investigate the Cl^- Shannon ionic radii domain.[50]

■ RESULTS AND DISCUSSION

Identification of Redox Reactions. The cyclic voltammograms of a $[\mathrm{Cation}]_2[\mathrm{UCl}_6]$ (0.01M) solution in [Cation]$[\mathrm{Tf_2N}]$ are shown in Figure 1. $[\mathrm{Cation}]^+$ stands for the IL cation $[\mathrm{BuMeIm}]^+$, $[\mathrm{BuMe_2Im}]^+$, $[\mathrm{BuMePyr}]^+$, or $[\mathrm{MeBu_3N}]^+$. Two main redox systems are observed around 0.2 and −2.2 V attributed, respectively, to the U^{V}/U^{IV} and U^{IV}/U^{III} couples according to the refs 40 and 43. The cyclic voltammograms of the $U^{IV}Cl_6^{2-}$ solution in the four ILs are recorded at various potential scan rates (ν) (Supporting Information, Figure S1 in $[\mathrm{BuMeIm}][\mathrm{Tf_2N}]$; Figure S2 in $[\mathrm{BuMe_2Im}][\mathrm{Tf_2N}]$; Figure S3 in $[\mathrm{BuMePyr}][\mathrm{Tf_2N}]$; Figure S4 in $[\mathrm{MeBu_3N}][\mathrm{Tf_2N}]$). The plots of anodic and cathodic peak intensities for the main redox systems observed versus the square root of ν give straight lines (Figures S5 and S6, Supporting Information). Furthermore, the anodic and cathodic peak potentials are almost constant with ν for the U^{V}/U^{IV} couple, while they vary for the U^{IV}/U^{III} couple. The peak to peak separation (ΔE_p) is reported for each redox couple in the four ILs (Table S1, Supporting Information). The values measured with our electrochemical device for the well-known ferricinium/ferrocene (Fc^+/Fc) redox system are also reported in the Table S1, Supporting Information. At 60 °C, ΔE_p of Fc^+/Fc (involving a reversible monoelectronic transfer)[51] is equal to the theoretical value 66 mV in $[\mathrm{BuMeIm}][\mathrm{Tf_2N}]$, the less viscous IL, and to 71 mV in $[\mathrm{MeBu_3N}][\mathrm{Tf_2N}]$, the most viscous IL. This increase in the ΔE_p value with the IL viscosity could be related to an increasing difficulty to correctly compensate the solution resistance. Indeed, the conductivity of ILs decreases with increasing viscosity.[1,51] Since the ΔE_p values of U^{V}/U^{IV} are equal to the Fc^+/Fc ones, U^{V}/U^{IV} can be regarded as a reversible system. Concerning the U^{IV}/U^{III} redox couple, ΔE_p increases from 73 mV in $[\mathrm{BuMeIm}][\mathrm{Tf_2N}]$ to 107 mV in $[\mathrm{MeBu_3N}][\mathrm{Tf_2N}]$. The U^{IV}/U^{III} system would be reversible in $[\mathrm{BuMeIm}][\mathrm{Tf_2N}]$ and would become quasi-reversible in $[\mathrm{MeBu_3N}][\mathrm{Tf_2N}]$. Therefore, both redox reactions involve monoelectronic transfer without changing the stoichiometry in chloride ligand and without coupling chemical reaction. As it was already reported in the ILs $[\mathrm{BuMeIm}][\mathrm{Tf_2N}]$, $[\mathrm{BuMe_2Im}][\mathrm{Tf_2N}]$, and $[\mathrm{MeBu_3N}][\mathrm{Tf_2N}]$, the uranium(IV) hexachloro complex could either be oxidized into $U^{V}Cl_6^-$ (eq 13) or reduced into $U^{III}Cl_6^{3-}$ (eq 14) in the four studied ILs.[40,43] This is an important result since the uranium(V) species generally undergoes chemical reaction leading to the formation of a dioxo uranium(V) complex. From these results, the uranium hexachloro complexes appear as an ideally suited system to study the interaction between anionic species with different charges and IL cations by an electrochemical technique.

$$U^{IV}Cl_6^{2-} \rightarrow U^{V}Cl_6^{-} + 1e^- \tag{13}$$

$$U^{IV}Cl_6^{2-} + 1e^- \rightarrow U^{III}Cl_6^{3-} \tag{14}$$

Furthermore, an ill-defined cathodic peak around 0 V relative to the U^{V}/U^{IV} system is observed at the reverse scan. This redox process can be observed for hexachloro uranium solution in the four ILs selected for this study (see, for example, Figure S7, Supporting Information, the cyclic voltammograms in $[\mathrm{BuMeIm}][\mathrm{Tf_2N}]$ and $[\mathrm{MeBu_3N}][\mathrm{Tf_2N}]$). Moreover, the intensity of this cathodic peak depends on the water content (data not shown). This observation may be related to the stability of uranium(V) species. Indeed, uranium(V) chloro complexes undergo rapid hydrolysis and disproportionation.[46,52] We have then assumed that in presence of water, the uranium(V) hexachloro complex can be partially hydrolyzed into the dioxo uranium(V) complex $U^{V}O_2Cl_4^{3-}$ leading to the post cathodic peak on the cyclic voltammograms (Figure 1 and Figure S7, Supporting Information). This result shows that even in presence of some amount of water, a uranium(V) species without oxygen bonding, that is, a non-dioxo compound, can be observed in ILs.

Moreover, a small cathodic peak is also observed from −1.4 to −1.5 V and is associated with the small anodic peak from −0.36 to 0 V depending on the IL (the anodic peak is not observed if the potential is first scanned in the positive direction). The magnification of the curves is reported in the Figure S8, Supporting Information. According to the electrochemical behavior of tetrachloro uranyl(VI) complexes in ILs,[53] these peaks can be attributed to the reduction of $[U^{VI}O_2Cl_4]^{2-}$. The presence of a small amount of uranyl(VI) in the hexachloro complex of uranium(IV) results likely from an oxidation by the atmospheric oxygen during the synthesis. The

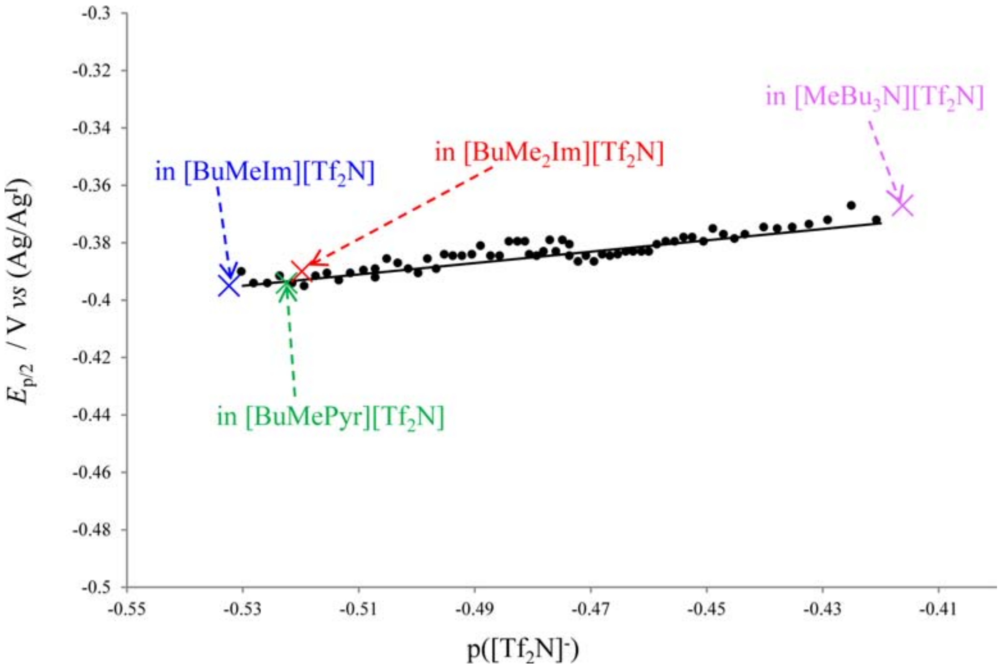

Figure 2. Standard potential (estimated by $E_{p/2}$) variation of the redox system Fc^+/Fc (0.01 M) in the mixture of ILs [MeBu$_3$N][Tf$_2$N] and [BuMeIm][Tf$_2$N] as a function of the $[Tf_2N]^-$ concentration at 60 °C at 0.1 V s^{-1}.The standard potentials in the pure [BuMeIm][Tf$_2$N] (blue ×); [BuMePyr][Tf$_2$N] (green ×); [BuMe$_2$Im][Tf$_2$N] (red ×); and [MeBu$_3$N][Tf$_2$N] (purple ×) ILs are reported on the graph at the corresponding p([Tf$_2$N]$^-$).

uranium(IV) hexachloro complexes at the solid state have been analyzed by time-resolved laser fluorimetry spectroscopy (Figure S9, Supporting Information). The emission spectra of uranium(IV) compounds present the same bands as the ones observed for a tetrachlorouranyl(VI) solution in ILs.

While the cyclic voltammograms of the uranium solution in the four ILs present the same redox system, Figure 1 provides evidence of some differences. First, the peak intensities reported in Table 1 depend on the IL. The ILs having different viscosities (Table 1), the diffusion coefficients and so the peak currents depend on the solvent.[40,51] Second, the redox potentials measured in the various ILs (Table 1) are different. We have to notice that the cathodic peak potential for the redox couple U^V/U^{IV} can be correctly measured even when the small postpeak is observed in reduction. In our previous study on the electrochemical behavior of $U^{IV}Cl_6^{2-}$ in ILs, the half-peak potential of the $U^{IV}Cl_6^{2-}/U^{III}Cl_6^{3-}$ and $U^VCl_6^-/U^{IV}Cl_6^{2-}$ systems in [MeBu$_3$N][Tf$_2$N] are reported to be negatively shifted 250 and 80 mV, respectively, in [BuMeIm][Tf$_2$N].[40] This reveals a strong interaction via the formation of ion pairs between uranium anionic species and IL cations, this interaction being stronger with [BuMeIm]$^+$ than with [MeBu$_3$N]$^+$. The magnitude of the potential shift reflects the strength of the interaction: the ion pairing effect would be stronger in the $U^{IV}Cl_6^{2-}/U^{III}Cl_6^{3-}$ system than in the $U^VCl_6^-/U^{IV}Cl_6^{2-}$ one. This can be related to the overall negative charge of the $U^{III}Cl_6^{3-}$ higher than that of $U^VCl_6^-$. Such potential shifts have already been observed with organic compounds[22−30] and oxygen[31−39] in pure ILs or in molecular solvents containing ILs as supporting electrolyte. A stabilization of the electrogenerated anionic species by interaction with the IL cations results in a shift toward the positive potentials. These ion pairings can occur by H-bonding, $\pi-\pi$, or electrostatic interactions. The cation−anion interaction strength depends mainly on the charge of the solute: monoanions would be less affected by ion pairing than dianions. But the ion pairing magnitude is also function of the IL cation nature (that is the structure, the size, the steric hindrance, and the distribution of charge). For example, the 1-butyl-3-methylimidazolium is described as a highly electropositive cation and its planar structure allows a closer approach to the anions than bulky cations like the tetraalkylammonium ones.[28] The magnitude of the ion pairing between the anionic electroactive species and the IL cations can be quantified from the potential shift. In the case of the electroreduction of dioxygen, the magnitude of ion pairing between the 1-ethyl-3-methylimidazolium cation [EtMeIm]$^+$ and $O_2^{\bullet-}$ and O_2^{2-} has been evaluated by cyclic voltammetry.[35] The authors have considered an association reaction between the IL cation and the electrogenerated species (eq 15). The association constant has been measured by using an expression depending on the apparent standard potential of the redox couple $O_2/O_2^{\bullet-}$. The association constant for $O_2^{\bullet-}$−EtMeIm$^+$ (13.5) is comparable to the one for $O_2^{\bullet-}$−H_2O (15.7). The authors have then concluded that $O_2^{\bullet-}$−EtMeIm$^+$ ion pairing is strong and that the process is similar to a complexation reaction.

$$O_2^{\bullet-} + \mathrm{EtMeIm}^+ \rightleftarrows O_2^{\bullet-}\text{—}\mathrm{EtMeIm}^+ \qquad (15)$$

Study of the Fc$^+$−[Tf$_2$N]$^-$ Ion Pairing. The protocol for studying the interaction between ionic species and the IL ions is first tested with ferrocene. The electrochemical behavior of Fc is well-known. Its oxidation involving one electron leads to the formation of the ferricinium cation (Fc$^+$). Assuming the formation of an ion pair between the cationic form Fc$^+$ and the anion of IL, the redox reaction can be written as

$$\mathrm{Fc} + x[\mathrm{Tf_2N}]^- \rightarrow \mathrm{Fc(Tf_2N)}_x^{\,1-x} + 1e^- \qquad (16)$$

The corresponding expression of potential is given by

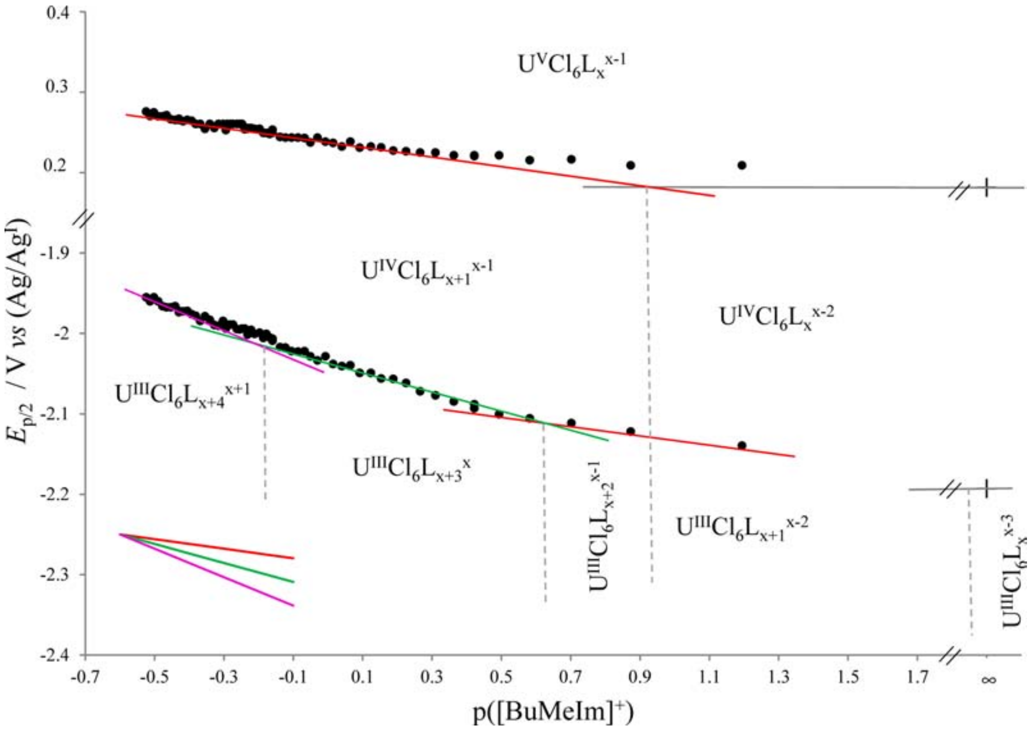

Figure 3. Predominance diagram for hexachloro uranium species (0.01 M) in the IL $[MeBu_3N][Tf_2N]$ at 25 °C, as a function of the potential and the $[BuMeIm]^+$ concentration. $E_{p/2}$ is measured by cyclic voltammetry $((E_{pa} + E_{pc})/2)$ at 0.1 V s^{-1} for a $U^{IV}Cl_6^{2-}$ (0.01 M) solution in $[MeBu_3N][Tf_2N]$ with increasing amounts of a $U^{IV}Cl_6^{2-}$ (0.01 M) solution in $[BuMeIm][Tf_2N]$. The standard potential of U^V/U^{IV} and U^{IV}/U^{III} in $[MeBu_3N][Tf_2N]$ (+) is reported on the graph at an arbitrary positive pL value. The slopes of the lines are 0.059 (red), 0.118 (green), and 0.177 mV/pL (purple).

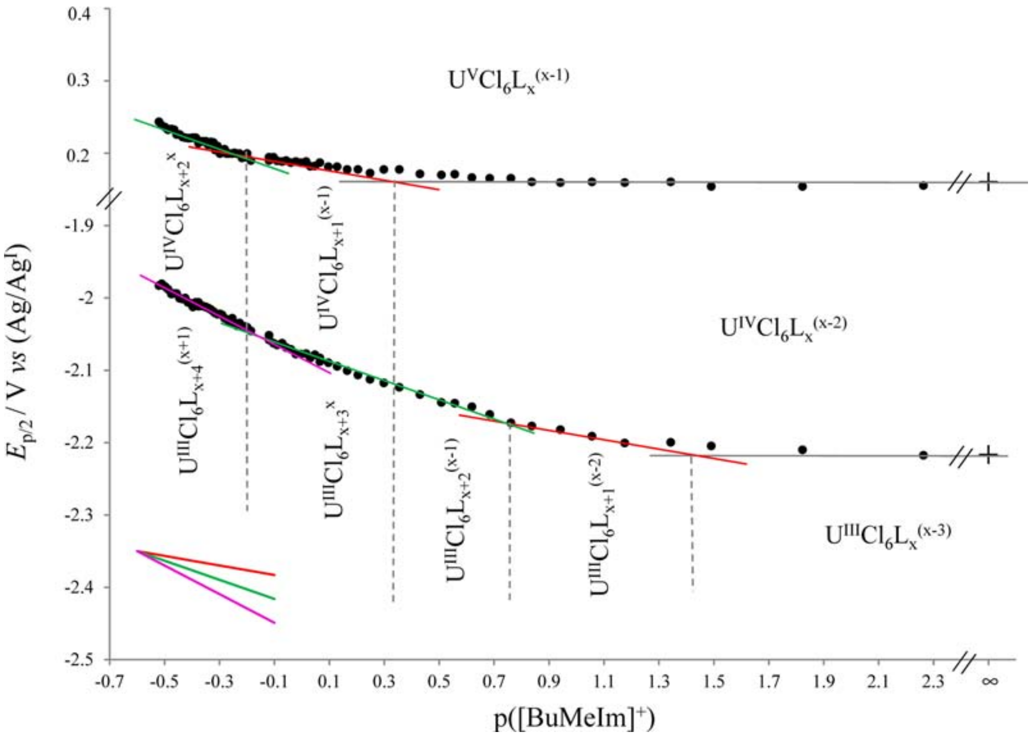

Figure 4. Predominance diagram for hexachloro uranium species (0.01 M) in the IL $[MeBu_3N][Tf_2N]$ at 60 °C, as a function of the potential and the $[BuMeIm]^+$ concentration. $E_{p/2}$ is measured by cyclic voltammetry $((E_{pa} + E_{pc})/2)$ at 0.1 V s^{-1} for a $U^{IV}Cl_6^{2-}$ (0.01 M) solution in $[MeBu_3N][Tf_2N]$ with increasing amounts of a $U^{IV}Cl_6^{2-}$ (0.01 M) solution in $[BuMeIm][Tf_2N]$. The standard potentials of U^V/U^{IV} and U^{IV}/U^{III} in $[MeBu_3N][Tf_2N]$ (+) are reported on the graph at an arbitrary positive pL value. The slopes of the lines are 0.066 (red), 0.132 (green), and 0.198 mV/pL (purple).

$$E'^0 = E^0 + 2.303\frac{RT}{F}x\,\mathrm{p}([\mathrm{Tf_2N}]^-) \qquad (17)$$

The number of IL anions $[Tf_2N]^-$ associated with Fc^+ can thus be calculated by measuring the standard potential of the Fc^+/Fc redox couple as a function of the $[Tf_2N]^-$ concentration. For that purpose, E'^0 is estimated by the half sum of the anodic (E_{pa}) and cathodic (E_{pc}) peak potentials ($E_{p/2}$), E_{pa} and E_{pc} being measured from cyclic voltammograms registered on Fc solution in different mixtures of [BuMeIm]-$[Tf_2N]$ and $[MeBu_3N][Tf_2N]$ ILs. The range of $[Tf_2N]^-$ concentration investigated lies between 2.62 and 3.38 mol·L^{-1} (Table 1). The graph reported Figure 2 is a straight line with a slope of 200 mV/p($[Tf_2N]^-$), corresponding at 60 °C to a difference of three anions in the first coordination sphere between Fc^+ and Fc. We can then conclude that the measurement of the standard potential as a function of the IL ion concentration is a suitable protocol to estimate the number of IL ions associated with electroactive ionic species.

Extent of the Uranium Species–$[BuMeIm]^+$ Ion Pairing. The predominance diagram of the uranium(III, IV, V) hexachloro species in ILs is established according to the protocol described in the Experimental Section. The use of the Nernst equation to calculate the potential standard is valid in the case of a reversible system, as for U^V/U^{IV}. In the case of U^{IV}/U^{III}, a quasi-reversible system, the value of E^0 can be regarded as estimation. However, the quasi-reversible feature is pronounced in ammonium IL, in the right part of the diagram. The variation of the standard potentials of U^V/U^{IV} and U^{IV}/U^{III} systems are reported Figure 3 as a function of the $[BuMeIm]^+$ concentration in the $[MeBu_3N][Tf_2N]$ IL at 25 °C. Both curves can be divided into segments having slopes proportional to 2.3 RT/F, namely, 0.059, 0.118, and 0.177 V/pL for a difference of one, two and three IL cations, respectively, at 25 °C. The increase in the segment slope from 0 to 0.059, 0.059 to 0.118, and 0.118 to 0.177 V/pL corresponds to the successive formation of species composed of hexachloro uranium(V), (IV), or (III) and IL cations. The difference in the IL cation number ($(x - y)$ for U^V/U^{IV} and $(y - z)$ for U^{IV}/U^{III}) can be determined between the oxidized and the reduced form of one redox couple by using eqs 9c and 10b relative to U^V/U^{IV} and U^{IV}/U^{III} systems, respectively.

By analogy with Pourbaix's diagram, the predominance diagram of the uranium hexachloro species has been built as a function of the $[BuMeIm]^+$ content.[54] The interactions $U^VCl_6^-$–$[BuMeIm]^+$ and $U^VCl_6^-$–$[MeBu_3N]^+$ have been assumed to be similar since identical total solute–solvent interaction energy values are reported by Schurhammer et al..[44] These authors have also calculated close values for the IL cation number in the first coordination sphere of $[U^VCl_6]^-$, 4.6 in $[BuMeIm][Tf_2N]$ and 4.1 in $[MeBu_3N][Tf_2N]$. Therefore, for the diagram reported in Figures 3 and 4, $U^VCl_6L_x^{x-1}$ has been assumed to be the predominant species for the upper potentials domain whatever the $[BuMeIm]^+$ concentration. Figure 3 shows that the number of $[BuMeIm]^+$ cations present in the first coordination sphere of $U^{IV}Cl_6^{2-}$ and $U^{III}Cl_6^{3-}$ increases with the $[BuMeIm]^+$ concentration. For the highest concentrated samples (left part of the graph), a difference of one cation is observed between $U^VCl_6^-$ and $U^{IV}Cl_6^{2-}$ and three cations between $U^{IV}Cl_6^{2-}$ and $U^{III}Cl_6^{3-}$. These results clearly provide evidence that the interaction between hexachloro uranium anionic species and IL cations is stronger with $[BuMeIm]^+$ than with $[MeBu_3N]^+$. Moreover, for a given value of p($[BuMeIm]^+$), the number of $[BuMeIm]^+$ in interaction with the uranium species increases in the following order: $U^{III}Cl_6^{3-} > U^{IV}Cl_6^{2-} > U^VCl_6^-$. This result confirms that the degree of ion pairing depends strongly on the charge of the compounds. Starting from the value of 4.6 $[BuMeIm]^+$ cations in the first coordination sphere of $U^VCl_6^-$ in $[BuMeIm][Tf_2N]$, we can then estimate a value of 5.6 and 8.6 cations in the coordination sphere of $U^{IV}Cl_6^{2-}$ and $U^{III}Cl_6^{3-}$, respectively. These values measured by electrochemical techniques at 25 °C are close to the ones calculated by molecular dynamics at 127 °C (5.5 for $U^{IV}Cl_6^{2-}$ and 7.6 for $U^{III}Cl_6^{3-}$).[44]

The temperature effect has also been studied by measuring the standard potential of the uranium redox systems at 60 °C as a function of p($[BuMeIm]^+$) in $[MeBu_3N][Tf_2N]$ solution (Figure 4). Some association constants defined by eqs 5 and 6 have been deduced from Figure 3 at 25 °C and from Figure 4 at 60 °C. These constants can be considered as a way to compare the strength of the ion pairing as function of the IL cations or the temperature. Since the diagram in Figures 3 and 4 can be considered as a Pourbaix's diagram, species on both sides of straight lines are in equilibrium and the change in the number of IL cation occurs at pL values corresponding to a slope modification. The association constants pK_i^{IV} and pK_i^{III} can therefore be estimated from these values. The so-determined association constants are reported in Table 2. The association constants measured at 60 °C are smaller than the ones at 25 °C. That means that the degree of ion pairing tends to decrease with temperature. The mechanism of the association reaction reported in eqs 1–3 involves different steps being all temperature-dependent, especially the IL cation transport from the bulk to the first coordination sphere and vice versa. Indeed, in our case, the $[BuMeIm]^+$ cations go from the bulk to the uranium first shell, while the $[MeBu_3N]^+$ cations go out of the first coordination sphere. Because the viscosity of $[BuMeIm][Tf_2N]$ (61 cP at 25 °C) is smaller than that of $[MeBu_3N][Tf_2N]$ (593 cP at 25 °C), the mass transport depends strongly on the IL. Moreover, the strength of the ion pairing depends on the IL ion dissociation, being directly related to the IL conductivity, which also depends on the temperature.[55] Therefore, the variation of the ion pairing magnitude with the temperature cannot be easily explained.

Table 2. Association Constants between the Hexachloro Uranium(III) and (IV) Species with the IL Cation $[BuMeIm]^+$ (25 °C), $[BuMePyr]^+$ (25 °C), and $[BuMeIm]^+$ (25 and 60 °C)

	$[BuMe_2Im]^+$ at 25 °C	$[BuMePyr]^+$ at 25 °C	$[BuMeIm]^+$ at 25 °C	$[BuMeIm]^+$ at 60 °C
pK_1^{IV}		0.65	1.09	0.32
pK_2^{IV}		−0.1		−0.2
pK_1^{III}	0.45	1.09	2.04	1.42
pK_2^{III}		0.18	1.1	0.76
pK_3^{III}			0.56	0.32
pK_4^{III}			−0.04	−0.2

Variation of the Interaction Strength As a Function of the IL Cation. To study the influence of the IL cations on the magnitude of the interaction with the uranium species, the same protocol (measurement of the standard potential as a function of the IL cations concentration) has been applied to $[BuMe_2Im]^+$ and $[BuMePyr]^+$ cations at 25 °C. Figure 5 represents the variation of the standard potential of the

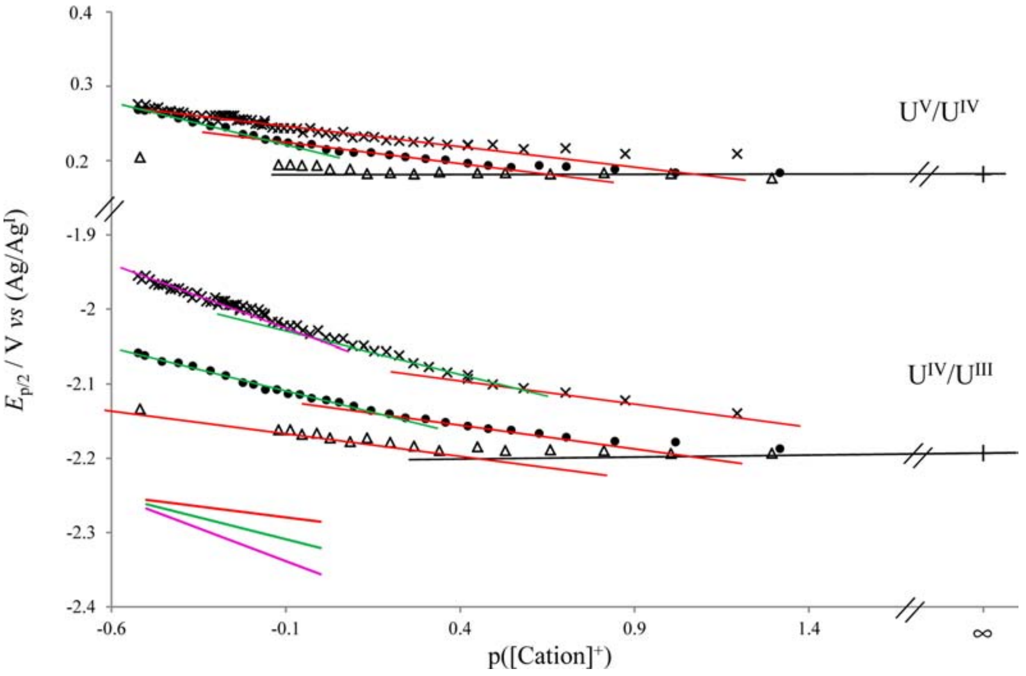

Figure 5. Variation of the standard potential (estimated by $E_{p/2}$) as a function of pL for the redox couples U^{V}/U^{IV} and U^{IV}/U^{III} at 25 °C. L represents the IL cations $[BuMeIm]^+$ (×); $[BuMePyr]^+$ (●), and $[BuMe_2Im]^+$ (Δ). $E_{p/2}$ is measured by cyclic voltammetry at 0.1 V s^{-1} for a $U^{IV}Cl_6^{2-}$ (0.01 M) solution in $[MeBu_3N][Tf_2N]$ with increasing amounts of a $U^{IV}Cl_6^{2-}$ (0.01 M) solution in [Cation]$[Tf_2N]$. The standard potentials of U^{V}/U^{IV} and U^{IV}/U^{III} in $[MeBu_3N][Tf_2N]$ (+) are reported on the graph at an arbitrary positive pL value. The slopes of the colored lines are 0.059 (red), 0.118 (green), and 0.177 mV/pL (purple).

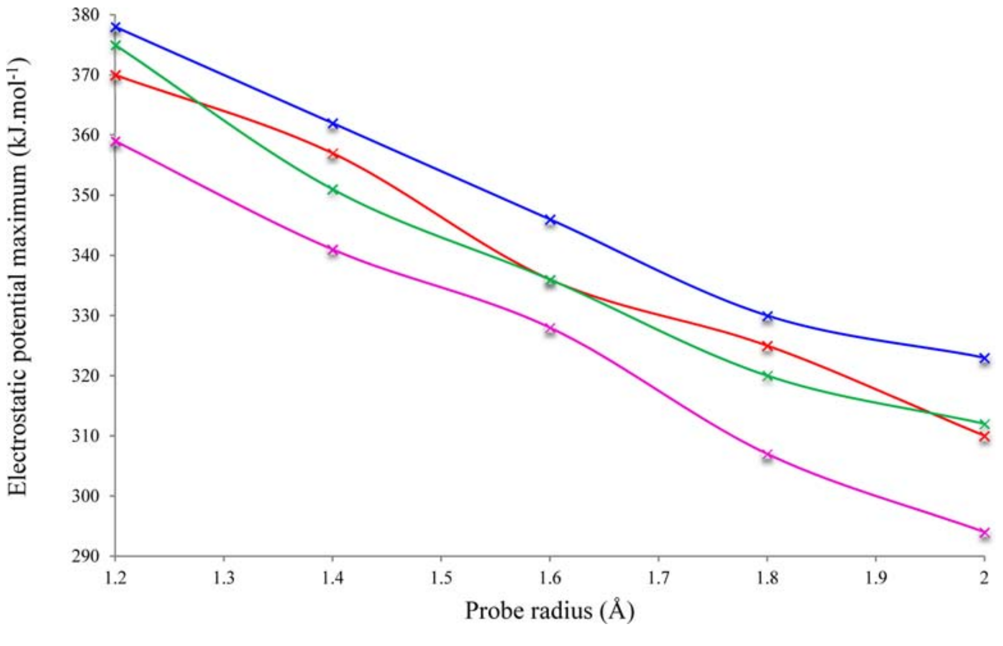

Figure 6. Electrostatic potential maximum energy (kJ mol^{-1}) as a function of the probe radius for $[BuMeIm]^+$ (blue), $[BuMe_2Im]^+$ (red), $[BuMePyr]^+$ (green), and $[MeBu_3N]^+$ (purple).

uranium redox couples as a function of the IL cation ($[BuMeIm]^+$, $[BuMePyr]^+$ and $[BuMe_2Im]^+$) concentration in $[MeBu_3N][Tf_2N]$. Whatever the IL cation, the curve can be divided into segments having slopes proportional to 0.059, 0.118, and 0.177 V/pL for respectively a difference of one, two and three IL cations at 25 °C.

Upon addition of $[BuMe_2Im]^+$ cations in $[MeBu_3N][Tf_2N]$ solution, the apparent standard potential does not vary significantly, unlike what it was observed with $[BuMeIm]^+$. The strength of the ion pairing between uranium hexachlo complexes and $[BuMe_2Im]^+$ is in the same order of magnitude as the one with $[MeBu_3N]^+$. This result confirms that the hydrogen on the C (C2) linked to the two nitrogen atoms plays an important part in the interaction with uranium complexes. This hydrogen, indeed, is the most acidic of the imidazolium ring. Strong association between $[BuMeIm]^+$ cations and the uranium chloro species would then occur by H-bonding, mainly with the carbon linked to both nitrogens. An intermediate situation is observed with $[\mathrm{BuMePyr}]^+$: the values of $E_{p/2}$ relative to U^{IV}/U^{III} increase with decreasing $\mathrm{p}([\mathrm{BuMePyr}]^+)$, and this potential is lower than the corresponding value in the presence of $[\mathrm{BuMeIm}]^+$ for the same pL value. While the $[\mathrm{BuMeIm}]^+$ cation is an aromatic ring with a delocalized charge, the $[\mathrm{BuMePyr}]^+$ cation is a nonaromatic ring with a charge localized on the nitrogen atom. As this latter atom is included in a ring and is linked to a butyl and a methyl chain, interaction with this cation is weakened due to steric hindrance. Therefore, the interaction between uranium hexachloro complexes and IL cations depends on the charge of the anionic species, the charge dispersion on the IL cation, and the steric effect.

The association constants $\mathrm{p}K_i^{\mathrm{IV}}$ and $\mathrm{p}K_i^{\mathrm{III}}$ estimated from Figure 5 are reported in Table 2. For a given oxidation state, the pK value depends on the IL nature and follows this order: $\mathrm{p}K_{[\mathrm{BuMeIm}]^+} > \mathrm{p}K_{[\mathrm{BuMePyr}]^+} > \mathrm{p}K_{[\mathrm{BuMe_2Im}]^+}$. Moreover, for a given IL cation, the constant is greater for the uranium(III) complex than for the uranium(IV) one. These results thus highlight that the interactions involving the anionic uranium species depend both on the IL cation ($[\mathrm{BuMeIm}]^+ > [\mathrm{BuMePyr}]^+ > [\mathrm{BuMe_2Im}]^+$) and on the global charge of the uranium hexachloro species ($U^{III}Cl_6^{3-} > U^{IV}Cl_6^{2-}$).

Ab initio calculations are then carried out to evaluate the strength of the interaction between the IL cations and the anionic uranium species. The electrostatic potential on anionic accessible surfaces is determined with probe radii varying from 1.2 to 2.0 Å for the four IL cations. The maxima of the electrostatic interaction energy on these surfaces are plotted, for each IL cation, in Figure 6. First, these results confirm that $[\mathrm{BuMeIm}]^+$ and $[\mathrm{MeBu_3N}]^+$ are the IL cations that can interact the most and the least, respectively, with anionic species: whatever the probe radius, these two IL cations have electrostatic potential maximum higher or lower, respectively, than the others. Furthermore, as already stated by Bossé et al.[43] and in good agreement with our electrochemical results, the ab initio calculations for $[\mathrm{BuMeIm}]^+$ provide evidence of the specific role of the proton linked to the C2 for the interaction with anions: the maximum of the electrostatic potential energy is located on this hydrogen. However, the electrostatic potential calculations for $[\mathrm{BuMePyr}]^+$ and $[\mathrm{BuMe_2Im}]^+$ do not allow us to draw a conclusion about these cations' electrostatic interaction skills toward the chloride of the UCl_6^{n-} anions since (i) the electrostatic potential maximum energies of these two IL cations are very close, and (ii) this energy is the highest for either $[\mathrm{BuMePyr}]^+$ or $[\mathrm{BuMe_2Im}]^+$ depending on the selected ionic radius probe between 1.2 and 2.0 Å.

■ CONCLUSIONS

Voltammograms of UCl_6^{2-} in four $[\mathrm{Tf_2N}]^-$ based ILs reveal two redox systems: a reversible system, $U^{V}Cl_6^{-}/U^{IV}Cl_6^{2-}$, and a quasi-reversible one, $U^{IV}Cl_6^{2-}/U^{III}Cl_6^{3-}$. Depending on the water content, the uranium(V) hexachloro complex, a non-dioxo U(V) species, is stable at least at the voltammetric time scale in the selected ILs.

The standard potential of both redox systems depends on the IL. This result has been attributed to specific interactions between the anionic uranium chloro complexes and the IL cations. The variation of the potential standard of $U^{V}Cl_6^{-}/U^{IV}Cl_6^{2-}$ and $U^{IV}Cl_6^{2-}/U^{III}Cl_6^{3-}$ redox systems as a function of the $[\mathrm{Cation}]^+$ concentration in $[\mathrm{MeBu_3N}][\mathrm{Tf_2N}]$ solution, $[\mathrm{Cation}]^+$ representing $[\mathrm{BuMeIm}]^+$, $[\mathrm{BuMe_2Im}]^+$, and $[\mathrm{BuMePyr}]^+$, allowed us to study the interaction between the anionic uranium(III, IV, V) species and the IL cations. From the predominance diagrams drawn for the uranium chloro complexes, we can conclude that (i) the magnitude of association increases with the uranium charge: $U^{V}Cl_6^{-} < U^{IV}Cl_6^{2-} < U^{III}Cl_6^{3-}$ and (ii) the strength of the interaction depends on the IL cation nature following this order: $[\mathrm{MeBu_3N}]^+ < [\mathrm{BuMe_2Im}]^+ < [\mathrm{BuMePyr}]^+ < [\mathrm{BuMeIm}]^+$. The ion pairing would occur by H-bonding between chloride of uranium complexes and IL cations and electrostatic interaction. Electrostatic potential energy is also calculated for the four IL cations. The results obtained by electrochemistry and ab initio calculations indicate that the cation ability for ion pairing depends on its electropositivity, its H-bonding ability, and its structure and size.

■ ASSOCIATED CONTENT

Ⓢ Supporting Information

Cyclic voltammograms of $U^{IV}Cl_6^{2-}$ solution in $[\mathrm{BuMeIm}][\mathrm{Tf_2N}]$, $[\mathrm{BuMe_2Im}][\mathrm{Tf_2N}]$, $[\mathrm{BuMePyr}][\mathrm{Tf_2N}]$, and $[\mathrm{MeBu_3N}][\mathrm{Tf_2N}]$ as a function of the potential scan rate at 60 °C, variation of the $U^{V}Cl_6^{-}/U^{IV}Cl_6^{2-}$ anodic peak intensity and $U^{IV}Cl_6^{2-}/U^{III}Cl_6^{3-}$ cathodic peak intensity versus the square root of the potential scan rate at 60 °C in the ILs $[\mathrm{BuMeIm}][\mathrm{Tf_2N}]$, $[\mathrm{BuMePyr}][\mathrm{Tf_2N}]$, $[\mathrm{BuMe_2Im}][\mathrm{Tf_2N}]$, and $[\mathrm{MeBu_3N}][\mathrm{Tf_2N}]$, cyclic voltammograms of a $U^{IV}Cl_6^{2-}$ solution in $[\mathrm{BuMeIm}][\mathrm{Tf_2N}]$ and $[\mathrm{MeBu_3N}][\mathrm{Tf_2N}]$, focusing on the postpeak in reduction for the U^{V}/U^{IV} system, magnification of the cyclic voltammograms of $U^{IV}Cl_6^{2-}$ solution in $[\mathrm{BuMeIm}][\mathrm{Tf_2N}]$, $[\mathrm{BuMe_2Im}][\mathrm{Tf_2N}]$, $[\mathrm{BuMePyr}][\mathrm{Tf_2N}]$, and $[\mathrm{MeBu_3N}][\mathrm{Tf_2N}]$ in the potential region [−2 V; 0 V], emission spectra of $[\mathrm{BuMeIm}]_2[U^{IV}Cl_6]$ in the solid state and of a $[\mathrm{BuMeIm}]_2[U^{VI}O_2Cl_4]$ solution in $[\mathrm{BuMeIm}][\mathrm{Tf_2N}]$. Values of the peak to peak separation of the $U^{V}Cl_6^{-}/U^{IV}Cl_6^{2-}$; $U^{IV}Cl_6^{2-}/U^{III}Cl_6^{3-}$ and Fc^+/Fc in the four ILs at 60 °C. This material is available free of charge via the Internet at http://pubs.acs.org.

■ AUTHOR INFORMATION

Corresponding Author

*Tel.: +33 169157152. Fax: +33 169157150. E-mail address: cannes@ipno.in2p3.fr.

Notes

The authors declare no competing financial interest.

■ ACKNOWLEDGMENTS

The authors thank the GNR PARIS (French organization) for their financial support.

■ REFERENCES

(1) Welton, T. *Chem. Rev.* **1999**, *99*, 2071−2084.
(2) Wilkes, J. S. *Green Chem.* **2002**, *4*, 73−80.
(3) Wasserscheid, P.; Keim, W. *Angew. Chem., Int. Ed.* **2008**, *39*, 3772−3789.
(4) Marsh, K. N.; Brennecke, J. F.; Chirico, R. D.; Frenkel, M.; Heintz, A.; Magee, J. W.; Petets, C.; Rebelo, L. P. N.; Seddon, K. R. *Pure Appl. Chem.* **2009**, *81*, 781−828.
(5) Plechkova, N. V.; Seddon, K. R. *Methods and Reagents for Green Chemistry: An Introduction*; Wiley-Interscience: New York, 2007.
(6) Soriano, A. N.; Doma, B. T.; Li, M. H. *J. Chem. Thermodyn.* **2009**, *41*, 301−307.
(7) Sundermeyer, W. *Angew. Chem., Int. Ed.* **1965**, *4*, 222−238.
(8) Kruesi, W. H.; Fray, D. J. *Metall. Trans. B* **1993**, *24*, 605−615.
(9) Hallett, J. P.; Welton, T. *Chem. Rev.* **2011**, *111*, 3508−3576.
(10) Kubisa, P. *Prog. Polym. Sci.* **2009**, *34*, 1333−1347.

(11) Lu, J.; Yan, F.; Texter, J. *Prog. Polym. Sci.* **2009**, *34*, 431−448.

(12) Olivier-Bourbigou, H.; Magna, L.; Morvan, D. *Appl. Catal. A: Gen.* **2010**, *373*, 1−56.

(13) Ohno, H. *Electrochemical Aspects of Ionic Liquids*; Wiley-Interscience: New York, 2005.

(14) Rogers, R. D., Seddon, K. R., Eds. *Ionic Liquids, Industrial Applications to Green Chemistry*; ACS Symposium Series 818; American Chemical Society: Washington, DC, 2002.

(15) Cocalia, V. A.; Gutowski, K. E.; Rogers, R. D. *Coord. Chem. Rev.* **2006**, *250*, 755−764.

(16) Binnemans, K. *Chem. Rev.* **2007**, *107*, 2592−2614.

(17) Solomon, E. I.; Hedman, B.; Hodgson, K. O.; Dey, A.; Szilagyi, R. K. *Coord. Chem. Rev.* **2005**, *249*, 97−129.

(18) Mandal, S.; Kazmi, N. H.; Sayre, L. M. *Arch. Biochem. Biophys.* **2005**, *435*, 21−31.

(19) Yamagata, M.; Tachikawa, N.; Katayama, Y.; Miura, T. *Electrochim. Acta* **2007**, *52*, 3317−3322.

(20) Matsumiya, M.; Suda, S.; Tsunashima, K.; Sugiya, M.; Kishioka, S.; Matsuura, H. *J. Electroanal. Chem.* **2008**, *62*, 129−135.

(21) Li, G.; Camaioni, D. M.; Amonette, J. E.; Conrad Zhang, Z.; Johnson, T. J.; Fulton, J. L. *J. Phys. Chem. B* **2010**, *114*, 12614−12622.

(22) Fry, A. J. *J. Electroanal. Chem.* **2003**, *546*, 35−39.

(23) Lagrost, C.; Carrié, D.; Vaultier, M.; Hapiot, P. *J. Phys. Chem. A* **2003**, *107*, 745−752.

(24) Lagrost, C.; Gmouth, S.; Vaultier, M.; Hapiot, P. *J. Phys. Chem. A* **2004**, *108*, 6175−6182.

(25) Brooks, C. A.; Doherty, A. P. *J. Phys. Chem. B* **2005**, *109*, 6276−6279.

(26) Cruz, H.; Gallardo, I.; Guirado, G. *Electrochim. Acta* **2008**, *53*, 5968−5976.

(27) Zigah, D.; Ghilane, J.; Lagrost, C.; Hapiot, P. *J. Phys. Chem. B* **2008**, *112*, 14952−14958.

(28) Nikitina, V. A.; Nazmutdinov, R. R.; Tsirlina, G. A. *J. Phys. Chem. B* **2011**, *115*, 668−677.

(29) Zhao, S.-F.; Lu, J.-X.; Bond, A. M.; Zhang, J. *Chem.—Eur. J.* **2012**, *18*, 5290−5301.

(30) Abdul-Rahim, O.; Simonov, A. N.; Rüther, T.; Boas, J. F.; Torriero, A. J.; Collins, D. J.; Perlmutter, P.; Bond, A. M. *Anal. Chem.* **2013**, *85*, 6113−6120.

(31) Buzzeo, M. C.; Klymenco, O. V.; Wadhawan, J. D.; Hardacre, C.; Seddon, K. R.; Compton, R. G. *J. Phys. Chem. B* **2004**, *108*, 3947−3954.

(32) Katayama, Y.; Onodera, H.; Yamagata, M.; Miura, T. *J. Electrochem. Soc.* **2004**, *151*, A59−A63.

(33) Ghilane, J.; Lagrost, C.; Hapiot, P. *Anal. Chem.* **2007**, *79*, 7383−7391.

(34) O'Toole, S.; Pentlavalli, S.; Doherty, A. P. *J. Phys. Chem. B* **2007**, *111*, 9281−9287.

(35) Islam, Md. M.; Ohsaka, T. *J. Phys. Chem. C* **2008**, *112*, 1269−1275.

(36) Barnes, A. S.; Rogers, E. I.; Streeter, I.; Aldous, L.; Hardacre, C.; Wildgoose, G. G.; Compton, R. G. *J. Phys. Chem. C* **2008**, *112*, 13709−13715.

(37) Islam, Md. M.; Imase, T.; Okajima, T.; Takahashi, M.; Niikura, Y.; Kawashima, N.; Nakamura, Y.; Ohsaka, T. *J. Phys. Chem. A* **2009**, *113*, 912−916.

(38) Rogers, E. I.; Huang, X.-J.; Dickinson, E. J. F.; Hardacre, C.; Compton, R. G. *J. Phys. Chem. C* **2009**, *113*, 17811−17823.

(39) Zigah, D.; Wang, A.; Lagrost, C.; Hapiot, P. *J. Phys. Chem. B* **2009**, *113*, 2019−2023.

(40) Nikitenko, S. I.; Cannes, C.; Le Naour, C.; Moisy, P.; Trubert, D. *Inorg. Chem.* **2005**, *44*, 9497−9505.

(41) Nikitenko, S. I.; Moisy, P. *Inorg. Chem.* **2006**, *45*, 1235−1242.

(42) Nikitenko, S.; Hennig, C.; Grigoriev, M.; Le Naour, C.; Cannes, C.; Trubert, D.; Bossé, E.; Moisy, P. *Polyhedron* **2007**, *26*, 3136−3142.

(43) Bossé, E.; Den Auwer, C.; Berthon, C.; Guilbaud, P.; Grigoriev, M. S.; Nikitenko, S.; Le Naour, C.; Cannes, C.; Moisy, P. *Inorg. Chem.* **2008**, *47*, 5746−5755.

(44) Schurhammer, R.; Wipff, G. *J. Phys. Chem. B* **2007**, *111*, 4659−4668.

(45) Bard, A. J.; Faulkner, L. R. *Electrochemical Methods, Fundamental and Applications*, 2nd ed.; Wiley: New York, 2001.

(46) Morss, L. R.; Edelstein, N. M.; Fuger, J. *The Chemistry of the Actinide and Transactinide Elements*, 3rd ed.; Springer: Dordrecht, the Netherlands, 2006; Vol. *1*.

(47) Frisch, M. J.; Trucks, G. W.; Schlegel, H. B.; Scuseria, G. E.; Robb, M. A.; Cheeseman, J. R.; Montgomery, J. A., Jr.; Vreven, T.; Kudin, K. N.; Burant, J. C.; Millam, J. M.; Iyengar, S. S.; Tomasi, J.; Barone, V.; Mennucci, B.; Cossi, M.; Scalmani, G.; Rega, N.; Petersson, G. A.; Nakatsuji, H.; Hada, M.; Ehara, M.; Toyota, K.; Fukuda, R.; Hasegawa, J.; Ishida, M.; Nakajima, T.; Honda, Y.; Kitao, O.; Nakai, H.; Klene, M.; Li, X.; Knox, J. E.; Hratchian, H. P.; Cross, J. B.; Bakken, V.; Adamo, C.; Jaramillo, J.; Gomperts, R.; Stratmann, R. E.; Yazyev, O.; Austin, A. J.; Cammi, R.; Pomelli, C.; Ochterski, J. W.; Ayala, P. Y.; Morokuma, K.; Voth, G. A.; Salvador, P.; Dannenberg, J. J.; Zakrzewski, V. G.; Dapprich, S.; Daniels, A. D.; Strain, M. C.; Farkas, O.; Malick, D. K.; Rabuck, A. D.; Raghavachari, K.; Foresman, J. B.; Ortiz, J. V.; Cui, Q.; Baboul, A. G.; Clifford, S.; Cioslowski, J.; Stefanov, B. B.; Liu, G.; Liashenko, A.; Piskorz, P.; Komaromi, I.; Martin, R. L.; Fox, D. J.; Keith, T.; Al-Laham, M. A.; Peng, C. Y.; Nanayakkara, A.; Challacombe, M.; Gill, P. M. W.; Johnson, B.; Chen, W.; Wong, M. W.; Gonzalez, C.; Pople, J. A. *Gaussian 03*, revision D.02; Gaussian, Inc.: Wallingford, CT, 2003.

(48) Besler, B. H.; Merz, K. M.; Kollman, P. A. *J. Comput. Chem.* **1990**, *11*, 431.

(49) Varetto, U., Molekel 5.4; Swiss National Supercomputing Centre, Lugano, Switzerland.

(50) Shannon, R. D. *Acta Crystallogr.* **1976**, *A32*, 751−767.

(51) Hapiot, P.; Lagrost, C. *Chem. Rev.* **2008**, *108*, 2238−2264.

(52) Selbin, J.; Ortego, J. D. *Chem. Rev.* **1969**, *69*, 657−671.

(53) Sornein, M.-O.; Cannes, C.; Le Naour, C.; Mendes, M.; Hennig, C. *J. Electroanal. Chem.* **2011**, *661*, 49−56.

(54) Pourbaix, M. J. N. Thermodynamique des Solutions Aqueuses Diluées: Représentation Graphique du Rôle du pH et du Potentiel, Ph.D. Thesis, Delft, The Netherlands, 1945; translation by Agar, J. N., published as Thermodynamics of Dilute Aqueous Solutions; Arnold: London, 1948.

(55) Andreussi, O.; Marzari, N. *J. Chem. Phys.* **2012**, *137*, No. 044508.